Materials Today: Proceedings 67 (2022) 577–590

Contents lists available at ScienceDirect

Materials Today: Proceedings

journal homepage: www.elsevier.com/locate/matpr

Genetic and particle swarm optimization algorithms based direct torque control for torque ripple attenuation of induction motor

Mohamed Elgbaily *, Fatih Anayi, Michael Packianather

Wolfson Centre for Magnetics, School of Engineering, Cardiff University, Cardiff, CF24 3AA, UK.

ARTICLE INFO

Article history:
Available online 5 September 2022

Keywords:
Genetic Algorithm
Particle Swarm Optimization
Direct Torque Control
Induction Motors

ABSTRACT

This paper introduces analysis, control, and comparison of two benchmarking optimization approaches called Genetic Algorithm (GA) and Particle Swarm Optimization (PSO) for Direct Torque Control (DTC) of a three-phase Induction Motor (IM). This study aims to determine the most efficient and robust of the two different metaheuristic optimization techniques including PID-PSO and PID-GA for DTC of IM. The purpose of the proposed control technique that has been presented is to get over the most significant drawback of DTC, which is a high level of torque output. The issue of torque ripples needs to be reduced to a significant amount using the two proposed control methods PSO-DTC and GA-DTC. As a result, PSO-DTC is the most applicable scheme. The proposed PID-PSO of DTC provided an excellent work performance for IM system drive. The comparison results of the suggested control methods showed a significant improvement of the control system compared to the classical DTC. The result is a high fidelity estimate of electromagnetic torque and speed for computation of motor parameters. A high ripple suppression capability was achieved by the PSO-DTC, which was measured at 22.5 % out of 47.28 % for the traditional approach. Both proposed control schemes were implemented using MATLAB/Simulink platform.

1. Introduction

The IMs are become widely used for changeable speed applications by using variable speed drives (VSD) for instance; pumps, crushers, blenders, saws, escalators, and derricks [1,2]. Beyond designing appropriate IMs in terms of security and the probability of energy reserving, induction motors are subjected to many investigations to achieve the best operational performance [3]. Many electrical loads are shared by induction motors, which are crucially characterised as preserving used energy and being highly effective [4]. Energy-saving is a major concern in electrical systems and is estimated correctly under different load conditions [5]. Likewise, the effectiveness of IM drive systems can be improved to operate the mechanical equipment with less energy usage at about 30 %, and it may also reduce the power demand by roughly 15 % [6].

Over the last decades, the majority of the VSD of IMs control techniques have been continuously upgraded and implemented in many types of applications, whether as motors or generators. The most commonly used IM control speed techniques are classified as Field Oriented Control (FOC) and Direct Torque Control (DTC) [7-9]. FOC has been classified as one of the best control techniques for the control of IMs. However, it mainly relies on the IM parameters which do need more control loops, such as a current regulator. This implementation complexity is the main drawback of FOC. In this case, the required control performance may not be achieved [8,10,11]. Moreover, DTC has been established to be a powerful control drive for IMs [12,13]. This control scheme has provided many features compared to FOC; fast torque response as the transient and steady-state torque conditions are much better than FOC technique. In addition, DTC does not need coordinate transformations, nor PI current regulators or a particular form of modulation techniques to generate pulse signals such as SVM or PWM. In the other hand, DTC suffers from many drawbacks like high torque ripples at low speed, variable switching frequency, and also the absence of direct current as a result, in harmonic losses and a high level of acoustic noise [14].

Many DTC control techniques have been developed in recent years to reduce the amount of torque ripples [15-17]. As a further matter, DTC has been modified to obtain constant switching frequency, such as Direct Torque Control with Space Vector Modula-

* Corresponding author.
E-mail address: elgbailymm@cardiff.ac.uk (M. Elgbaily).

https://doi.org/10.1016/j.matpr.2022.08.293

tion (DTC-SVM) [18] and Direct Mean Torque Control (DMTC) [19]. Furthermore, Artificial Intelligence (AI) strategies have been successfully employed in DTC and become acting instead of traditional strategies as referred in the literature review [20-22]. Fuzzy logic control (FLC) is one of the AI that has become a crucial component in the development of DTC [23]. It has been utilized whether on an outer loop as a speed control [24,25] or inner control loop using a membership function to create a switching table between the main three estimation variable of torque, flux, and flux angle [26,27]. FLC showed high work performance and robustness of IM drive system. However, the proposed model is slowing dwon the computational time [28]. Another control scheme of AI called Artificial Neural Network (ANN), a comparison work by [29] showed that the ANN approached better performance compared to DTC in terms of reducing torque ripple and also concluded that the Adaptive Neural-Fuzzy Inference System (ANFIS) model is technically superior to its system dynamics comparison with ANN. A comparison study presented by [30,31] regarding Sliding Mode Control (SMC) is also contributed to eliminating the drawback of DTC, space vectors was appropriately used via switching vectors table by using SMC.

All these mentioned contributions provided the improvement of the work performance of the DTC. In the meanwhile, the system leads to more complex of control schemes. Moreover, when performing in-depth analysis for these works, the DTC scheme appears to have lost one of its fundamental features. Although, the variety of the drawbacks of the DTC technique of induction motors in accordance with the literature review, the DTC is still efficiently employed in many applications due to its benefits by the nonexistence of:

- Coordination transformation
- PI regulator and current regulator
- Modulation signals PWM

The biggest challenge facing DTC is the torque ripple problem, particularly at the low speed range where it would lead to deteriorating performance of the system. This issue is generated from the switching table which is associated with the limit number of the selected vector during the duration of the sample period. In addition, the selection of voltage vector is dependent on the error and change of error signals of both torque and flux, which causes an inaccurate voltage vector selection.

The suggested strategy in this paper is to modify the optimal parameters of metaheuristic optimization approaches for GA and PSO for DTC of IM in order to obtain the most optimal values of the tuned PID controller gains. Dynamic modelling of IM was demonstrated and discussed. A concise explanation is given to demonstrate the fundamentals of conventional DTC design. Both optimization techniques, PSO and GA algorithms, have been enhanced to deliver a faster dynamic of torque while reducing torque ripple much more than traditional DTC. The implementation outcomes of the proposed strategies have been compared.

2. Modeling of induction motor

The necessity of an appropriate mathematical model of induction motor is required to facilitate the behavior study of the direct torque control model based on the expression of two-phase coordination $(d-q)$ [32]. Three phase induction motor drive can be generated under both dynamic and normal conditions. consequently, this model enables to determine the IM drive variable values such as stator and rotor current, stator and rotor voltage, stator and rotor flux, and electromagnetic torque. Afterword it is easily expressed a 3-phase induction motor drive to the differential equations form after transferring the main three phase quantities for stator and flux such as voltage, current, and flux. These quantities are transformed to two axis theory frame "d-q axis" or stationary frame by axis transformation as shown in Fig. 3(a). Equivalent circuit in "d-q axis" of IM drive is represented in Fig. 1, This was utilized to design this model and the stator and rotor quantities expressed as equations.

To refer the stator variables to a synchronously rotating reference frame fixed in the rotor, the park transformation is applied; as a result, the stator and rotor parameters rotate at synchronous speed, and all simulated variables in the stationary frame appear as DC quantities in the synchronously rotating reference frame. Table 6 in appendix A illustrates the IM parameters.

Representing the mathematical model of IM based on the form of $(d-q)$ is shown from Eq. (1) to Eq. (14) as follows:

- Electrical equations are from Eq. (1) to Eq. (8):

o voltages:

$$V_{ds} = R_s i_{ds} + \frac{d}{dt}\psi_{ds} \tag{1}$$

$$V_{qs} = R_s i_{qs} + \frac{d}{dt}\psi_{qs} \tag{2}$$

$$V_{dr} = R_r i_{dr} + \frac{d}{dt}\psi_{dr} - w_r \psi_{qr} \tag{3}$$

$$V_{qr} = R_r i_{qr} + \frac{d}{dt}\psi_{qr} + j w_r \psi_{dr} \tag{4}$$

o Current:

$$i_{ds} = \frac{\psi_{ds}(Ll_r + L_m) - \psi_{dr} L_m}{Ll_s Ll_r + Ll_s L_m + Ll_r L_m} \tag{5}$$

$$i_{qs} = \frac{\Psi_{qs}(Ll_r + L_m) - \Psi_{qr} L_m}{Ll_s Ll_r + Ll_s L_m + Ll_r L_m} \tag{6}$$

$$i_{dr} = \frac{\Psi_{dr}(Ll_s + L_m) - \Psi_{ds} L_m}{Ll_s Ll_r + Ll_s L_m + Ll_r L_m} \tag{7}$$

$$i_{qr} = \frac{\Psi_{qr}(Ll_s + L_m) - \Psi_{qs} L_m}{Ll_s Ll_r + Ll_s L_m + Ll_r L_m} \tag{8}$$

- Magnetic equations are from Eq. (9) to Eq. (12):

$$\Psi_{ds} = L_s i_{ds} + L_m i_{dr} \tag{9}$$

$$\Psi_{qs} = L_s i_{qs} + L_m i_{qr} \tag{10}$$

$$\Psi_{dr} = L_r i_{dr} + L_m i_{ds} \tag{11}$$

$$\Psi_{qr} = L_r i_{qr} + L_m i_{qs} \tag{12}$$

- Mechanical movement equations are represented in Eq. (13) for electromagnetic torque and Eq. (14) for rotor speed:

$$T_e = \frac{3}{2}\frac{P}{2}(i_{qs}\Psi_{ds} - i_{ds}\Psi_{qs}) \tag{13}$$

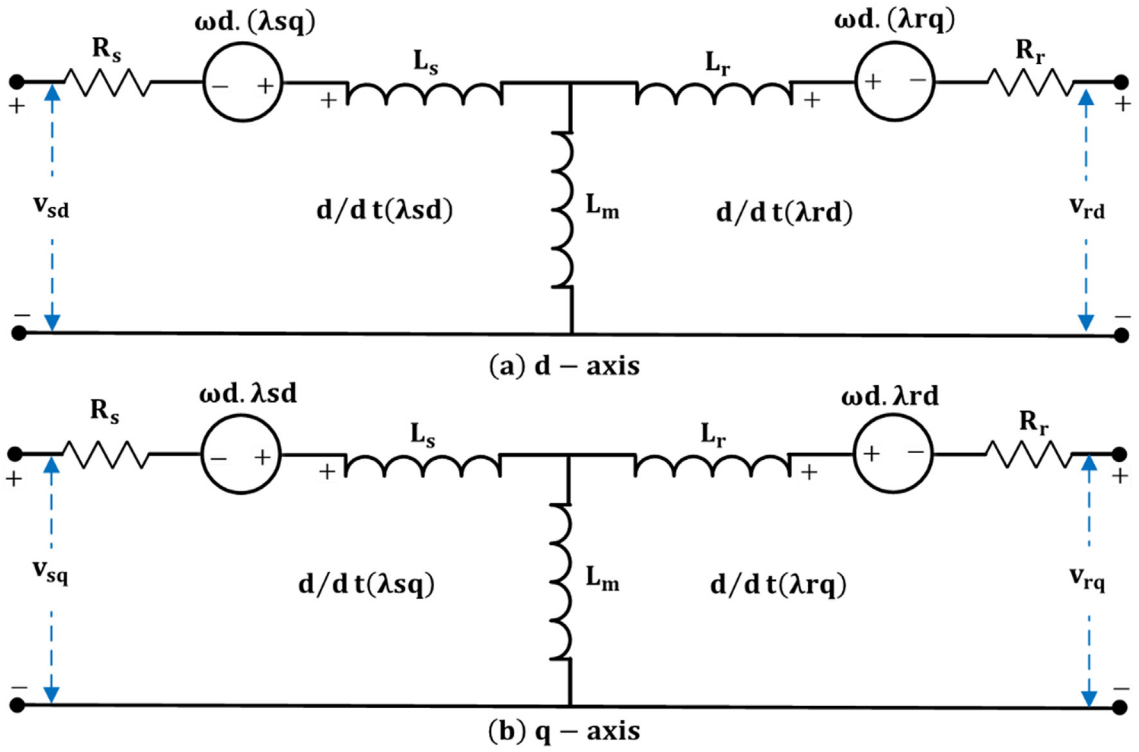

Fig. 1. The equivalent circuit of basic control scheme for DTC-IM based on "d-q axis".

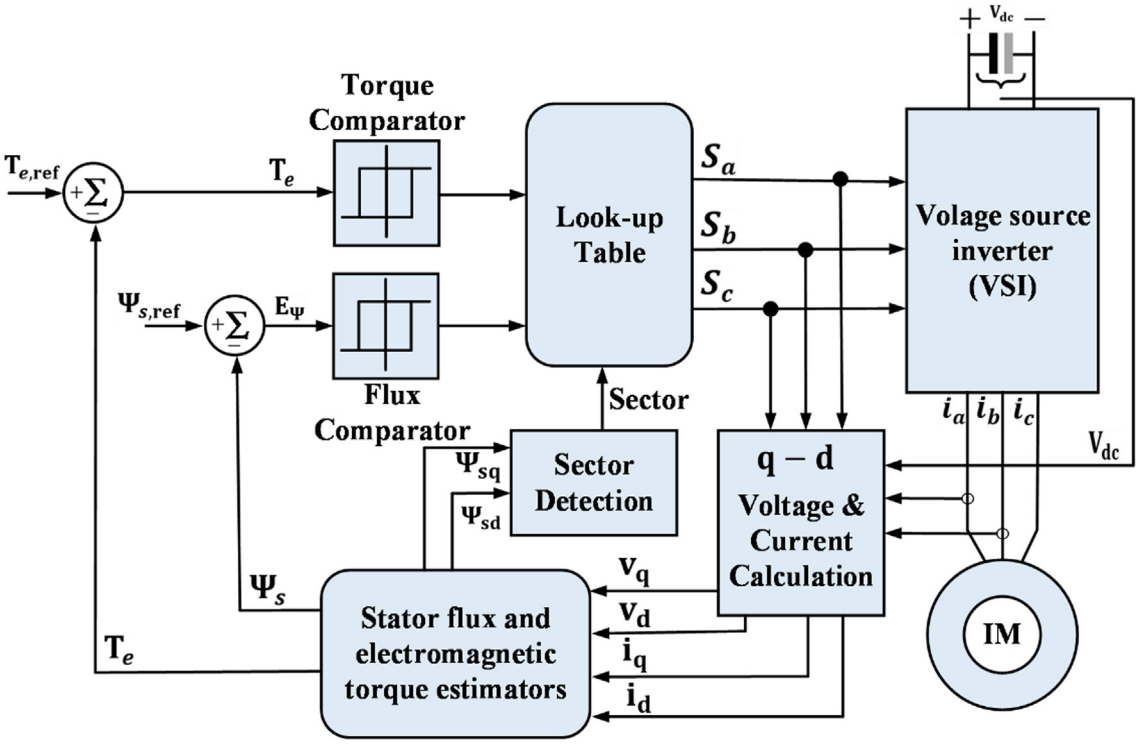

Fig. 2. The basic control scheme of DTC-IM.

$$\omega_r = \frac{P}{2J}\int (T_e - T_r) \tag{14}$$

Where:

- Stator resistor → R_s
- Rotor resistor → R_r
- Stator leakage inductance → Ll_s
- Rotor leakage inductance → Ll_r
- Mutual inductance → L_m

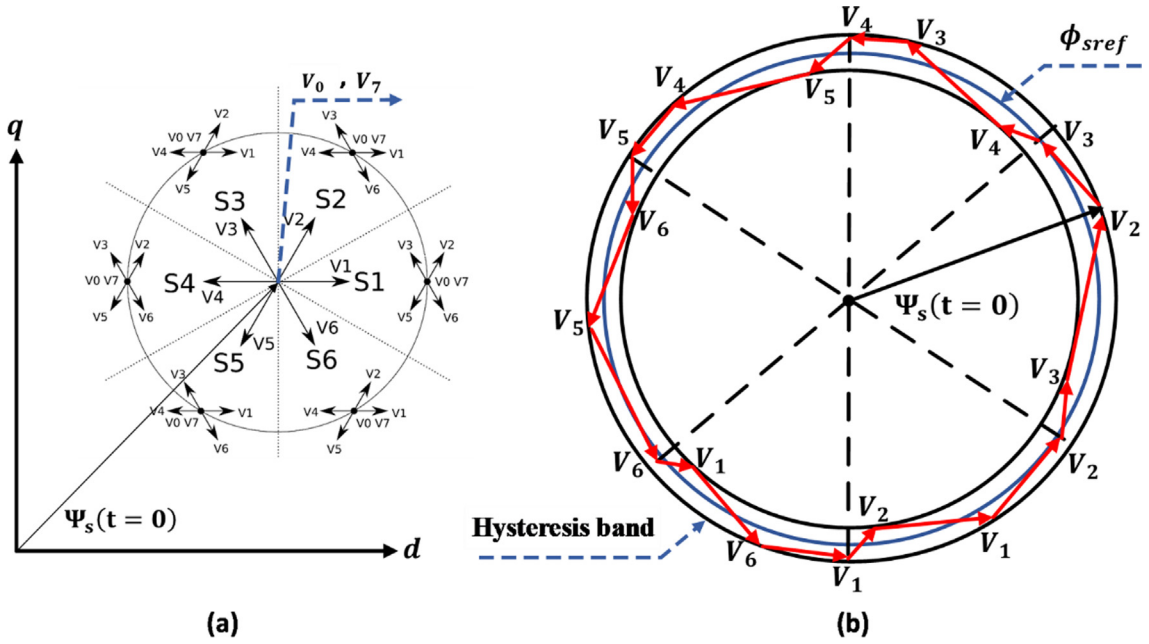

Fig. 3. (a) the trajectory space voltage vectors; (b) selecting space vectors based flux and torque changes.

Table 1
Switching table of conventional DTC.

ψ	T	Sector 1	Sector 2	Sector 3	Sector 4	Sector 5	Sector 6
	1	$V_2(110)$	$V_3(010)$	$V_4(011)$	$V_5(001)$	$V_6(101)$	$V_1(100)$
1	0	$V_7(111)$	$V_0(000)$	$V_7(111)$	$V_0(000)$	$V_7(111)$	$V_0(000)$
	−1	$V_6(101)$	$V_1(100)$	$V_2(110)$	$V_3(010)$	$V_4(011)$	$V_5(001)$
	1	$V_3(010)$	$V_4(011)$	$V_5(001)$	$V_6(101)$	$V_1(100)$	$V_2(110)$
0	0	$V_0(000)$	$V_7(111)$	$V_0(000)$	$V_7(111)$	$V_0(000)$	$V_7(111)$
	−1	$V_5(001)$	$V_6(101)$	$V_1(100)$	$V_2(110)$	$V_3(010)$	$V_4(011)$

Table 2
Applied and unapplied voltage vectors.

Sector	Applied Vectors	Unapplied Vectors
Sectors 1	V_0, V_2, V_3, V_5, V_6, V_7	V_1, V_4
Sectors 2	V_0, V_1, V_3, V_4, V_6, V_7	V_2, V_5
Sectors 3	V_0, V_1, V_2, V_4, V_5, V_7	V_3, V_6
Sectors 4	V_0, V_2, V_3, V_5, V_6, V_7	V_1, V_4
Sectors 5	V_0, V_1, V_3, V_4, V_6, V_7	V_2, V_5
Sectors 6	V_0, V_1, V_2, V_4, V_5, V_7	V_3, V_6

3. Conventional DTC

A very significant industrial contribution of DTC was introduced firstly by ABB company [33] just a few short years later of its invention by Takahashi [12]. The main feature of DTC scheme is that the torque and flux are controlled independently and directly by using the switching mode to select the optimal value of the voltage vector signal to run a voltage source inverter (VSI). DTC extremely depends on the estimation for actual values of both torque and

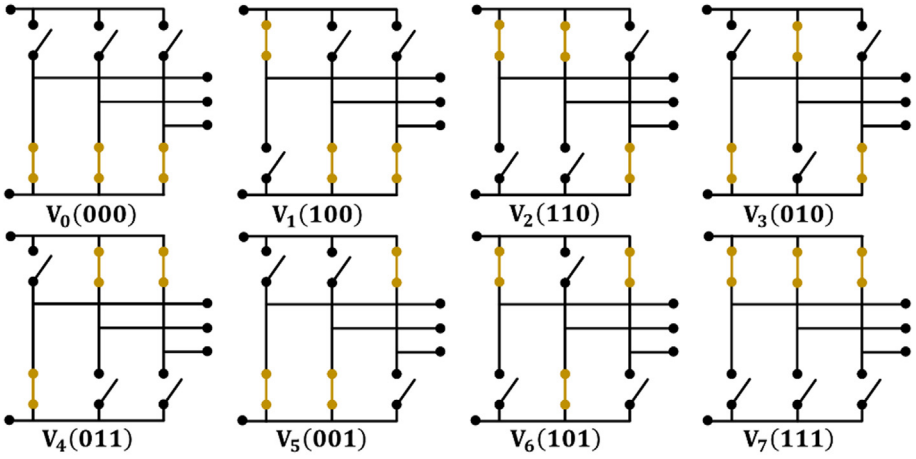

Fig. 4. Eight possible switching states of voltage source inverter.

flux. DTC is an inherently sensorless behavior control scheme; therefore, it is worth mentioning that the system is entirely neglected the parameters of rotor position for choosing the voltage vectors. There are two hysteresis controllers consists of switch off/on points considered as two levels. Its purpose is to redirect each flux vector in the space vector to be within the designated band of the hysteresis comparator. Torque direction can be controlled by the feature of two levels in the hysteresis control, they can provide whether negative or positive torque. Fig. 2 shows the fundamental design of DTC.

The output voltages of the inverter are based on control voltage space vectors as demonstrated in Fig. 3(a). The switching table is the main part of DTC to create flux orientation called space voltage vectors according to torque and flux error with taking into consideration the position of flux angle. The whole space vector area of the inverter is split into six sectors. These voltage vectors work as instantaneous values of eight vectors, six of them are active values, the other two are inactive which are equal to zero. Eq. (15) and Eq. (16) can approximate the variation of the stator flux.

$$\Delta\Psi_s = V_s \Delta t \tag{15}$$

$$\Psi_s = \Psi_{s0} + V_s \Delta t \tag{16}$$

Where: Ψ_{s0} is the stator flux at t = 0.

By choosing the proper voltage vectors, the stator flux Ψ_s can be maintained on the circle of constant flux, as indicated by the flux and torque sliding surfaces in Fig. 3(b). Likewise, torque angle δ is possibly decreased or increased according to the selection of voltage vector state as it is generating the torque control of IM based on (13).

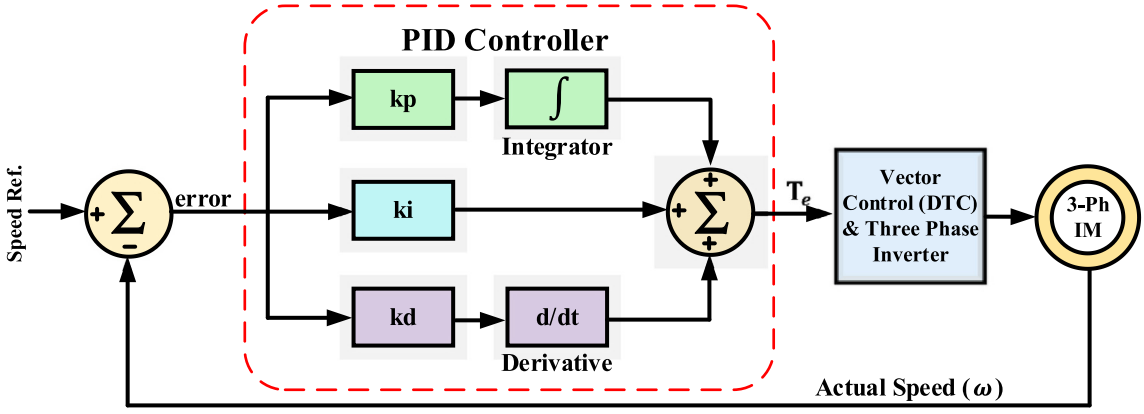

Fig. 5. Classical PID controller outer loop DTC drive system.

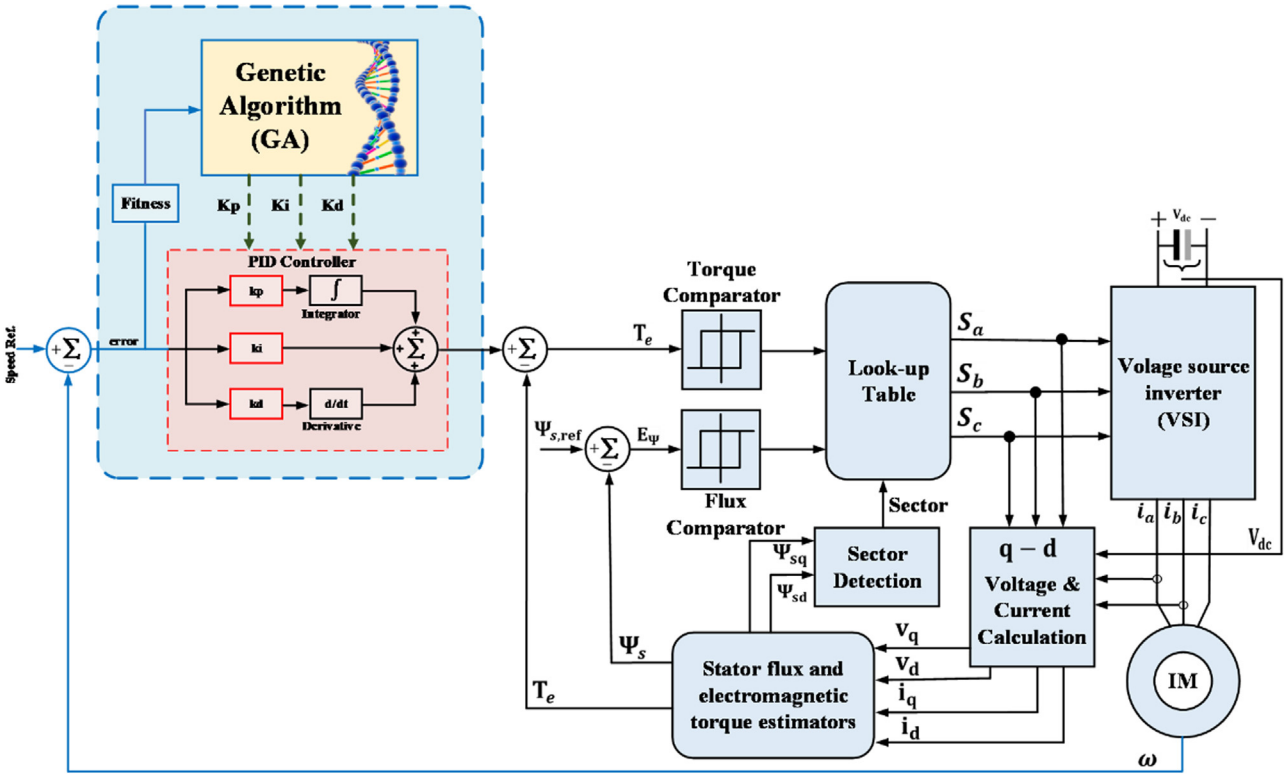

Fig. 6. The proposed GA-DTC algorithm.

Electromagnetic torque and stator flux are estimated as follows:

The stationary reference frame is referred to (q-d) the transformation from two to three-phase stator terminals of IM. According to stator voltages and DC bus voltages (V_{dc}) the switching state (S_a, S_b, S_c) are given in Eq. (22).

The estimation flux can be obtained as follows in Eq. (17) and Eq. (18):

$$\Psi_{ds} = \int V_{ds} - R_s i_{ds} \tag{17}$$

$$\Psi_{ds} = \int V_{ds} - R_s i_{ds} \tag{18}$$

Stator flux (ψ_s) can be determined by Eq. (5) to express as follows:

$$\psi_s = \sqrt{\psi_{ds}^2 + \Psi_{qs}^2} \tag{19}$$

The position of stator flux angle ($\theta_{\Psi s}$) is obtained by Eq. (20):

$$\theta = \measuredangle \Psi_s = \tan^{-1}\left(\frac{\Psi_{qs}}{\Psi_{ds}}\right) \tag{20}$$

The estimated electromagnetic torque can be derived by using the estimated components of current and flux which can be expressed by the following Eq. (21):

$$T_e = \frac{3}{2}\frac{P}{2}\left(i_{qs}\Psi_{ds} - i_{ds}\Psi_{qs}\right) \tag{21}$$

Table 1. shows a very simple switching table which is one of the fundamental parts of DTC. This table represents the sequence of selection voltage vectors. The actual voltage vector is selected with the aid of flux and torque hysteresis comparators with considering flux angle. This pattern of this table is depicted in Fig. 3. In this case, the work performance of the drive system is sufficient during the operating time of an induction motor.

Table 2. shows the applied voltage vectors based on the switching table of DTC. Each flux sector allows six voltage vectors to be as a final pulsating signal applied to the inverter taking the form of four active and two passive vectors.

In the other hand, the two-level inverter has been employed in the proposed control according to the switching states of the lookup table. The stator voltage vector V_s is entirely depends on the pulsating signals of S_a, S_b, and S_c, and can be summarised directly by Eq. (22) as following:

$$V_s = V_{sd} + jV_{sq} = \sqrt{\frac{2}{3}}V_{dc}\left(S_a + S_b e^{j(2/3)} + S_c e^{-j(2/3)}\right) \tag{22}$$

Where V_{dc} is the de link voltage of the inverter and V_{sd} and V_{sq} are the induced supply voltages of the three-phase induction motor.

Fig. 4, demonstrates the possible switching states of three phase inverter accordance to On-Off state of the converter semiconductor switches of IGBT device based on Eq. (22). Moreover, two of the eight states of the inverter switches are designated as zero voltage. Consequently, the stator flux will be zero volts, whereas the other six switches are distributed as shown in Fig. 3(a).(See Fig. 5 [32]).

4. PID controller

The PI controller has been widely used in industry sectors due to low cost, simple implementation and the capability to apply in a variety of applications of applications. In addition, it develops the dynamic response of the system in terms of eliminates or reduce the settling time error. It also reduces the overshoot and rise time response where the load changes to force the feedback to match a setpoint of the system. This can be achieved by providing an optimum value of proportional gain (K_p) using the error input signal with an integral component correction (K_i). The derivative response (K_d) is proportional to the rate of change of the process variable. The set value of most practical control systems uses very small derivative time (K_d) due to its response is highly sensitive to the process variable signal [34,40]. Eq. (23) shows the closed loop of DTC systm for IM accordance to PID controller.

$$u(t) = K_p e(t) + K_i \int_0^t e(t)dt + K_d \frac{(t)}{dt} \tag{23}$$

Where, u(t) is the output of the PID controller and e(t) is the error signal.

5. Proposed GA algorithm

off-line tuning algorithms are extremely challenging to deal with constant variations in the induction motor parameters where the nonlinearities that can be found in the inverter, the motor, and the controller, This makes on-line tuning of controllers is becoming increasingly popular in the engineering sector. The genetic algorithm (GA) is a simulation process utilizing computer computation

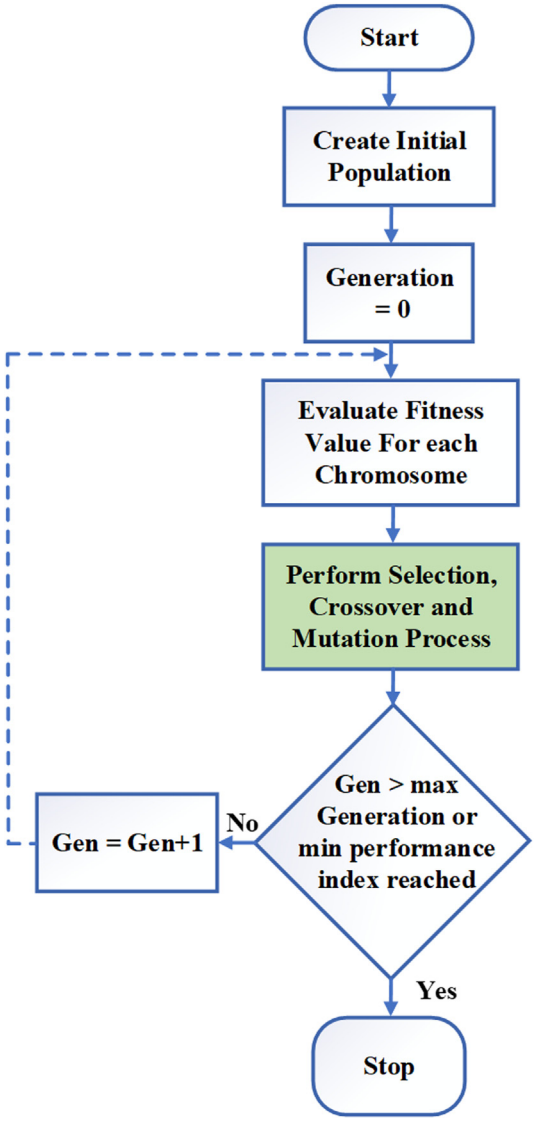

Fig. 7. Flowchart of GA algorithm.

that can associate with several concepts based on Mendel's work in genetics and Darwin's theory on natural selection and attempting the natural evolution of biological systems to be simulated. GA is an optimization tool that figures out several locations of the search space and can reveal multi-solution to solve an issue. it is an adoption of three main genetic variables: reproduction, crossover, and mutation. It was a significant contribution to the developing areas of engineering and other sciences. It was introduced firstly by John Holland and his colleagues in 1975 [34]. From the working principle of GA that mating and reproduction are the evolution candidates, whereas mutations are used to explore the total research space in order to prevent early confluence points. The work sequence of GA is shown in Fig. 7. (See Fig. 8).

The application of these three genetic operators is a repetitive process until stops at an optimal research solution toward the issue. Afterward, this optimal value is used as PID parameters to run the system online.

The modified drive system of DTC is shown in Fig. 1. The upgrading study was focused to reduce the torque ripples of DTC for induction motors which is a major issue of the classical design of DTC. PID is designed as a speed controller. The genetic Algorithm optimization tool is the main contribution of this modification for DTC. GA is one of the best solutions to provide an optimal value by tuning scaling factors of PID controller based on research strategy [35]. As the initial random population is the initiate generating parameters used in the simulation which going to be representing the PID controller for kp, ki and K_d is demonstrated in Table 5. Repetitive stimulation in an offline mode is the first step tuned by GA optimization tool using the gains of PID controller. Once the optimal value is found the PID gains can used online mode to control the IM speed throught out Eq. (23). Table 5. shows the obtained PID set using GA.

Fig. 6 is the block diagram for the proposed GA control scheme based on PID controller. In this case, GA is utilized to tune the PID gains (Kp, Ki and K_d) until the optimal control value is found. The aim of this process is to develop the DTC work performance in terms of reducing torque ripples. The simulation of GA algorithm is based on the initial random population of individuals which is acting as the parameters of PID controller gains as defined in Table 4.

The gains of PID controller are evaluated by GA tuning procure which is repeating the simulation in an offline mode to the best

Table 3
Parameters of PID upper and lower boundaries.

PID parameters	Kp	Ki	K_d
Maximum value	20	5	1
Minimum value	0	0	0

Table 4
Operators of meta-heuristic techniques used to determine the best PID gains settings.

Option	Number/type
Genetic algorithm	
No of variables	3
Limits boundaries	(0,0,0,15, 5, 1)
Population size	20
Maximum iteration	100
Crossover probability	0.8
Mutation probability	0.2
Fitness function	ITAE
Particle swarm optimization algorithm	
No of variables	3
Limits boundaries	(0,0,0,15, 5, 1)
No. Particles	15
Max iteration	100
Fitness function	ITAE
C1,C2	(2.4, 2.2)
Wmax	0.9
Wmin	0.2

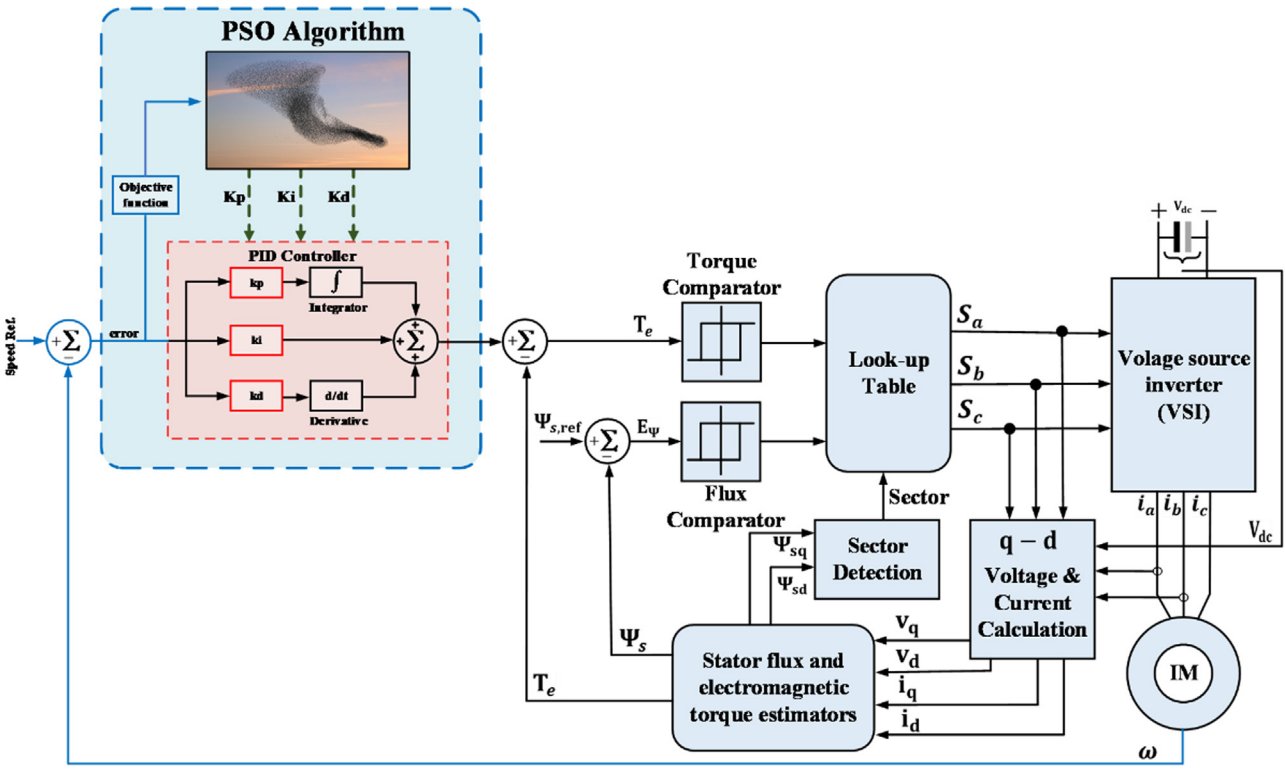

Fig. 8. The proposed PSO-DTC algorithm.

value of PID gains. Ultimately, if the optimal values are detected, they can be utilized to the online mode of the DTC scheme.

GA is particular category of evolutionary algorithms that incorporate strategies such as selection, crossover, and mutation that are inspired by evolutionary biology [23]. The sequences of GA operations as a flowchart are shown in Fig. 7, taking on to account which is a flowchart that adheres to the evolutionary principles of a GA.

6. Proposed PSO algorithm

Eberhart and Kennedy created the PSO algorithm in 1995 as one of many optimization strategies. This strategy, which is taken from social psychology, has been demonstrated to be resilient in solving issues with non-differentially and ono-linearity [36]. It was inspired by the social behavior and dynamic movement with communications of insects, birds flocking and fish schooling, and it has shown to be effective in addressing continuous nonlinear optimization problems. PSO is becoming more popular owing to its simplicity and ease of implementation [37,38]. The PSO method is superior to other stochastic approaches in terms of its ability to provide high-quality solutions in a shorter amount of time and with a more steady convergence characteristic. Because the PSO technique is an effective optimization methodology and a potential solution for handling the challenge of finding the best values for the PID controller settings [39].

Therefore, the PSO-PID controller, which searches to find the optimum PID values based on Eq. (23). This particular PID controller is developed and referred to as the PSO-PID controller.

Table 5
Optimum parameters of DTC gains by GA and PSO towards ITAE.

Tuned Parameters	PSO-DTC	GA-DTC	PSO-ITAE	GA-ITAE
Kp	9.43	11.23	9.6049	
Ki	0.1	2.3		9.8935
K_d	0.001	0.01		

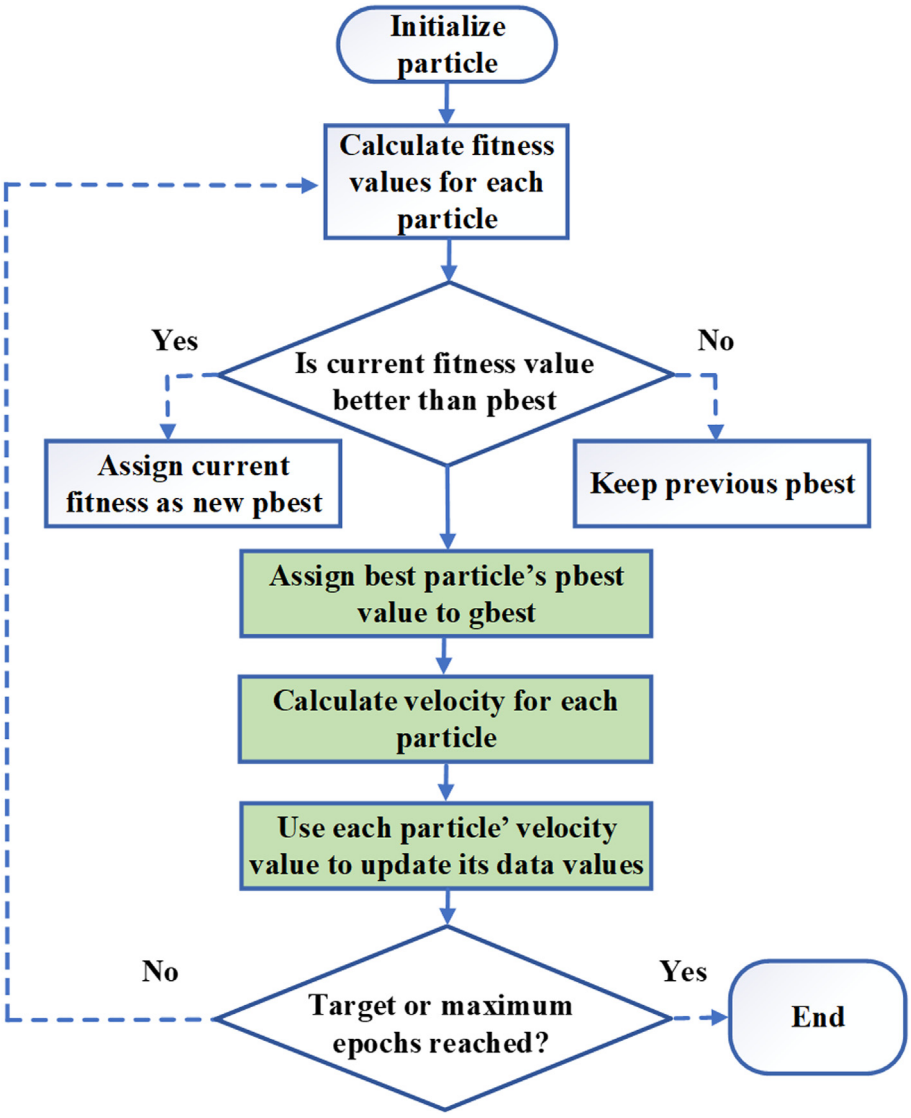

Fig. 9. Flowchart of PSO algorithm.

Each solution in PSO is a "bird" in the search space; this is referred to as a "particle." The swarm is represented as particles in a multi-dimensional space with locations and velocities. These particles must remember their optimal position and be recognize of the global best position. Members of a swarm communicate and move at high speeds depending on their best locations according to their flying experience with other particles. The particles are updated using the Eq. (24) and Eq. (25) below [40].

$$v_{i,j}(k+1) = w.v_{i,j}(k) + C_1 r_1\left(gbest - x(k)_{i,j}\right) + C_2 r_2\left(pbest_j - X(k)_{i,j}\right) \quad (24)$$

$$X(k+1)_{i,j} = x(k)_{i,j} + V(k)_{i,j} \quad (25)$$

Where:

$v_{i,j}$ is velocity.

i, j: are particle and dimension.

C_1, C_2 are acceleration constant (cognitive individual and social group) learning rate.

W is inertia weight factor.

r_1, r_2 are random numbers between 0 and 1.

pbest is the best position of a specific particle.

Gbest is the best particle position of the group.

From Eq. (24) the velocity of the swarm can be determined firstly by the previous speed is represented in $w.v_{i,j}(k)$ which is to prevent the particle from drastically changing the direction. The middle part of Eq. (24) is to make the particle tracks its best position $C_1 r_1\left(gbest - x(k)_{i,j}\right)$ the last part of Eq. (24) is to make the particle tracks the best position by found by the group as follows $C_2 r_2\left(pbest_j - X(k)_{i,j}\right)$.

Using the PSO method and a specified number of iterations, the software determines the final optimum value of the fitness function as "best fitness" and the last global optimal point as "gbest." Table 4. outlines the PSO parameters. Fig. 9 depicts the proposed PSO-DTC-IM flowchart.

7. Performance criteria of PSO and GA with PID controller

In most intelligent optimization algorithms, there are commonly performance criteria such as: integrated Absolute Error (IAE), the integrated of square error (ISE), and Integrated of Time Square Error (ITSE). That can be evaluated analytically in frequency domain. These performance criteria are including the overshoot, rise time, settling time and steady state error. Table 3. illustrates the boundaries of three variables for PID controller. In addition, it has been indicated the optimization, and robust of the drive system [41]. The performance criterion formulas are as follows:

$$ISE = \int_0^\infty e^2(t).dt \quad (26)$$

$$IAE = \int_0^\infty |e(t)|.dt \quad (27)$$

$$ITSE = \int_0^\infty t.e^2(t).dt \quad (28)$$

$$IATE = \int_0^\infty t.e^2(t).dt \quad (29)$$

In this study ITAE is employed as a fitness function for evaluating the performance of PID controller. According to objective functions that mentioned above in Eq. (29) that ITAE was provided the lowest error which can be classified as the best fitness function among others. The optimum tuned set values for K_p, K_i and K_d can yield a good step response to the proposed scheme. Table 4. demonstrates both operators of meta-heuristic techniques GA and PSO are modified to define the most optimum values for the scaling factor of PID controller. Table 4. Shows the optimum parameters of DTC gains that have achieved by using GA and PSO with selection of ITAE fitness function.

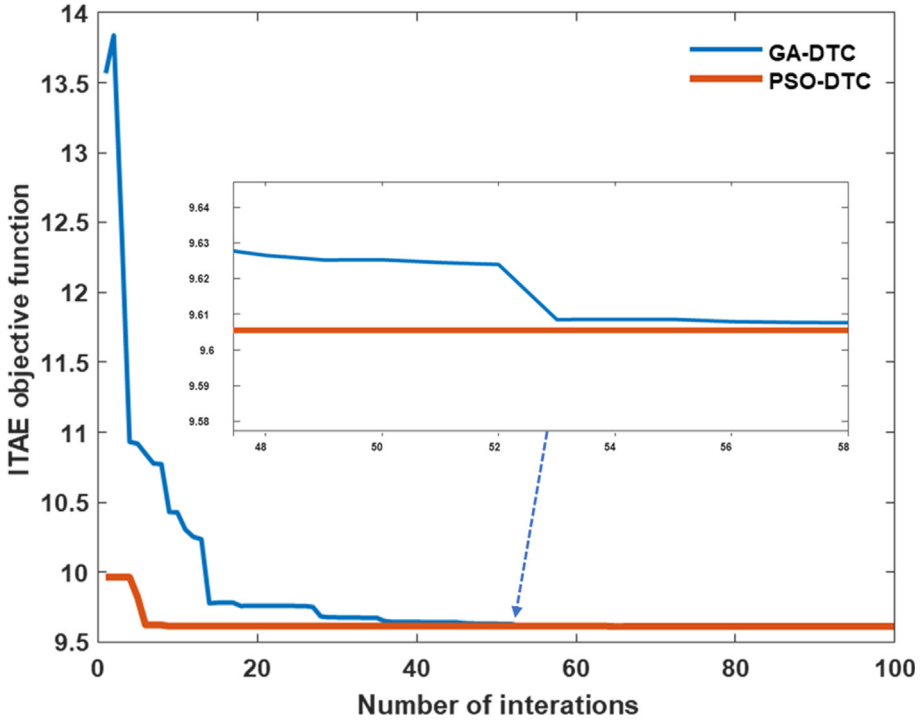

Fig. 10. Convergence characteristics of the GA and PSO tuned the proposed DTC design.

8. Simulation results and discussion

The main concern of this study is to investigate both proposed optimization tools namely GA and PSO of DTC-IM to be able to reduce a sufficient torque ripples issue under a wide range of torque loads. The proposed scheme control based on the GA algorithm has greatly declined the torque ripple by around 20 % compared to the conventional DTC. However, PSO was recorded the greatest reduction of torque ripples at roughly 25 % in accordance to the traditional DTC as shown in Fig. 11(a) and Fig. 14. The speed has shown a great response towards the torque loads. The transient and study state conditions have been improved dramatically for all variables, flux, torque, and speed. Fig. 11(b) is representing rotor speed; it is clearly shown the behavior of the transient state and steady state were significantly improved for both suggested PSO and GA schemes. However, the PSO was in the lead, which means the measured speed signal of the PSO was almost the same as the reference value for the entire period given compared to the GA algorithm. Fig. 12 (a) and (b) shows the current performance of the proposed schemes of DTC under a variable torque operation

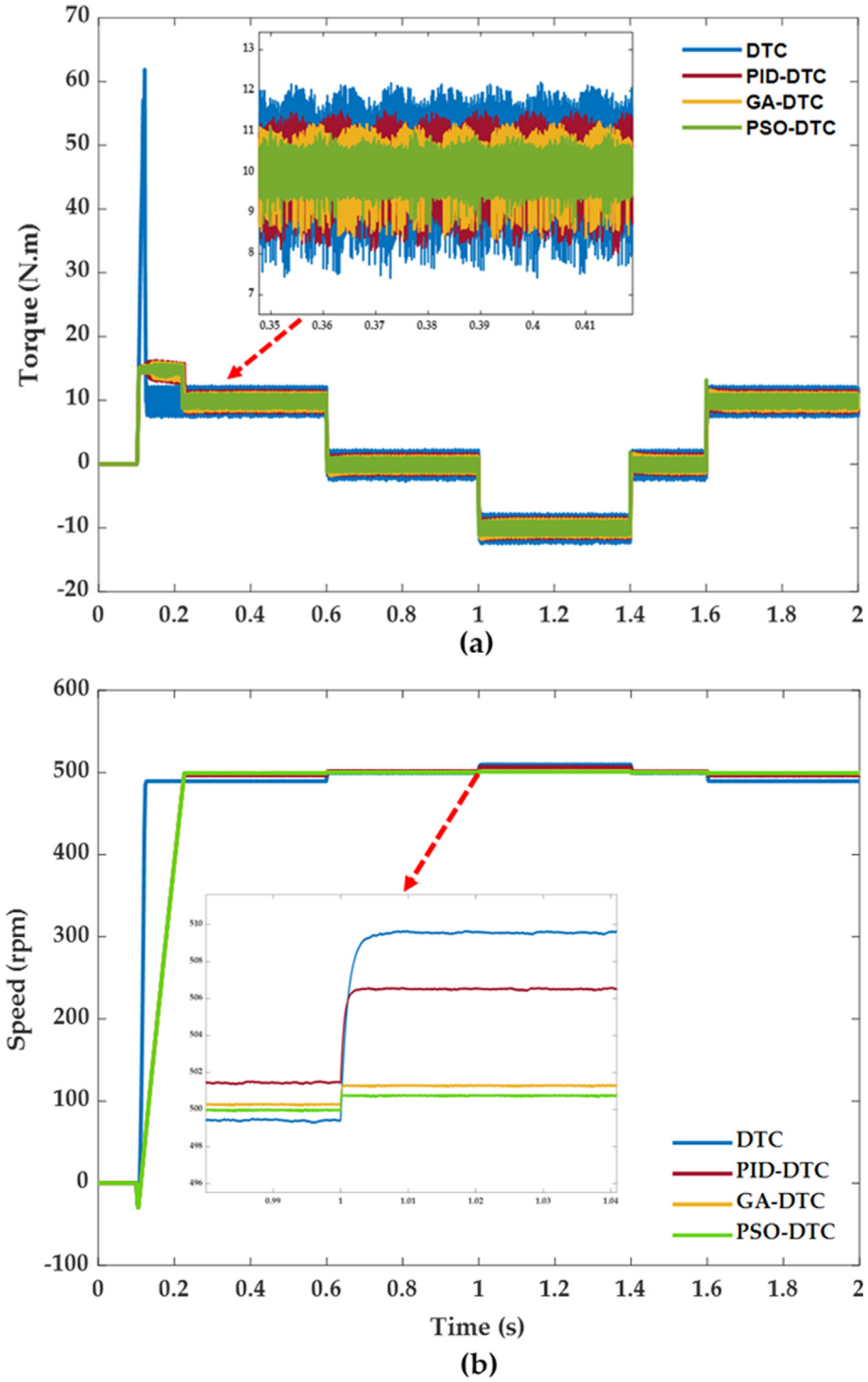

Fig. 11. (a) load torque responses; (b) rotor speed responses of the proposed PSO, GA, and PID towards the classical DTC.

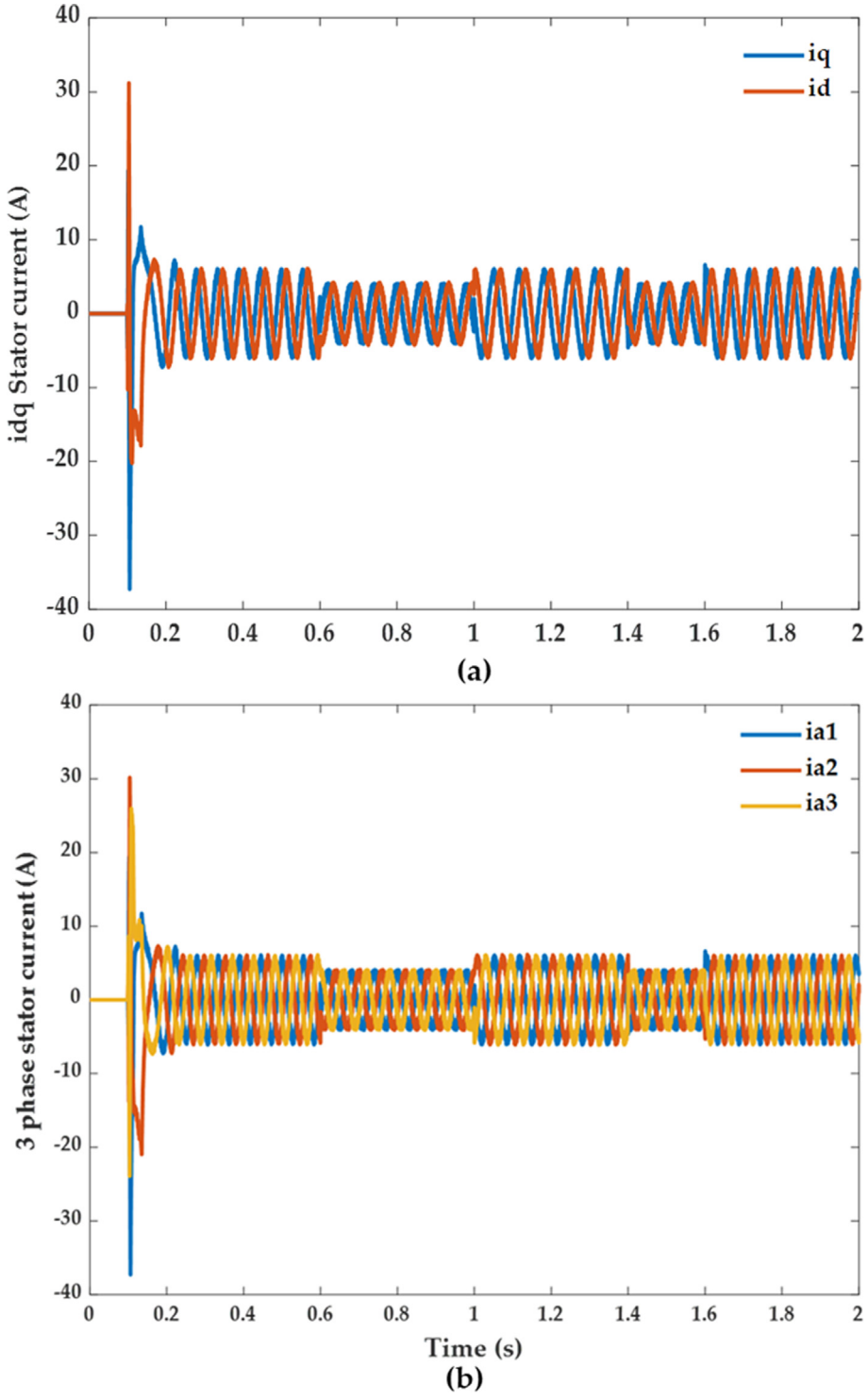

Fig. 12. (a) d-q axis stator current reference frame responses; (b) three-phase stator current responses.

for both; d-q axis stator current reference frame and three-phase stator current, respectively. Fig. 13 shows stator flux with excelent performance toward the proposed methods.

Fig. 10 is a convergence graph for GA and PSO algorithms. It is demonstrated the characteristics between GA and PSO algorithms based on DTC of three phase induction motor. From Fig. 10 it is observed that the PSO algorithm is slightly improved compared with GA algorithm.

Fig. 14 shows the percentage improvement of reducing torque ripples in DTC optimized by GA and PSO also demonstrate the proposed mothed was significantly reduced torque ripples compared to the conventional DTC. Also, it is observed that the total percentage of torque ripples of DTC is 47.28 % this amount of torque ripples was reduced gradually using classical PID, GA algorithm and PSO algorithm by 33.57 %, 28.19 % and 22.5 % respectively.

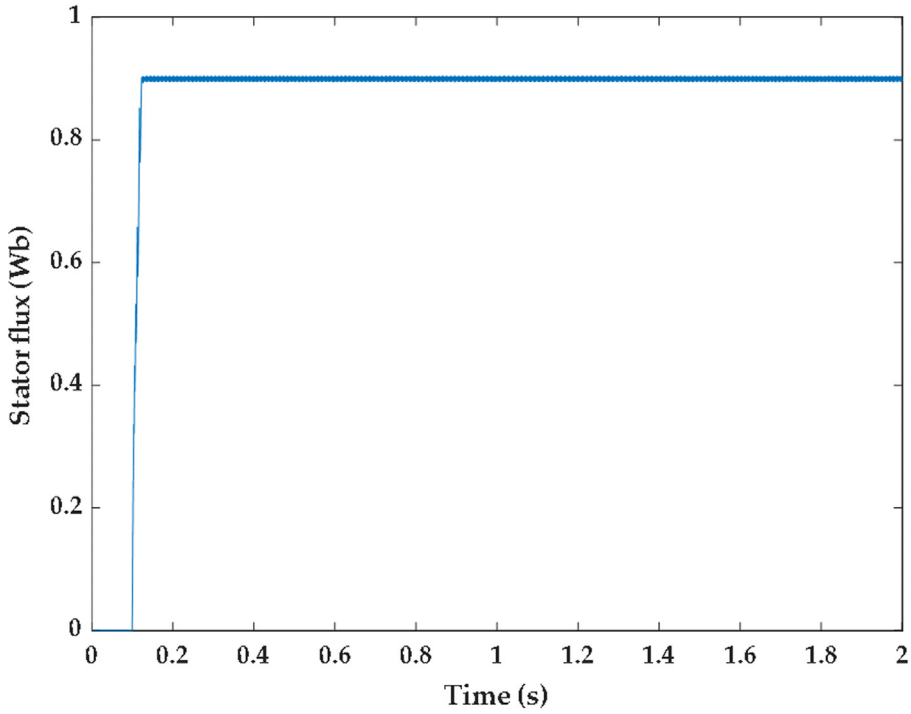

Fig. 13. Stator flux.

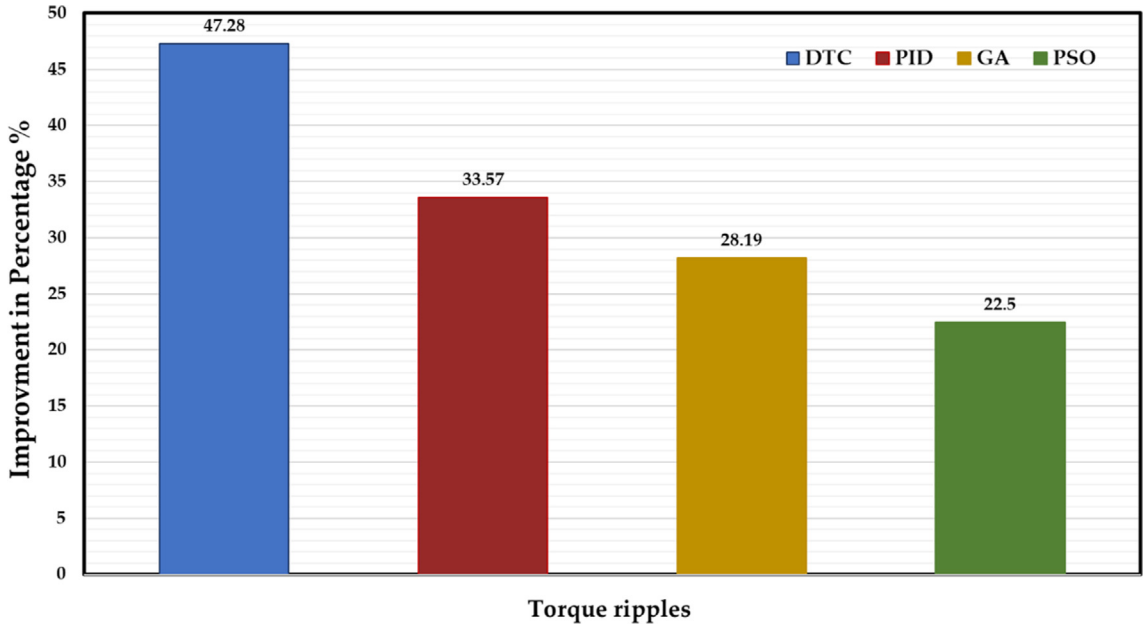

Fig. 14. Percentage of improvement in reducing torque ripples for DTC tuned by PID, GA and PSO.

9. Conclusion

This research offers two suggested GA and PSO optimization strategies for monitoring load conditions and reducing torque ripples in an IM direct torque control drive system. The GA and PSO algorithms have been utilized to obtain the best values for PID parameters. The achieved optimal values of PID gains gave a high dynamic performance of the DTC drive system. The results obtained from tuned PID by both GA and PSO algorithms are compared with PID-DTC and classical DTC. In simulation result, the GA-DTC and PSO-DTC reduced the torque ripple dramatically for a wide range of torque loads. Moreover, the developed drive system based on DTC has not lost any of its fundamentals compared to the work studies in the literature review.

The PSO was the best proposed scheme which reduced torque ripples to a great extent at about 1.9 N.m where it was in the conventional DTC at about 4.5 N.m. it was observed from the testbed of both proposed techniques that the PSO provides superior dynamic performance in terms of reducing torque ripples compared to second proposed GA scheme. The PSO recorded the attenuation of torque ripples at more than 25 % whereas GA has achieved only 20 % compared to the classical DTC. Consequently,

Table 6
Induction Motor Specifications.

Variables	Value	Unit
Rated power	2.1	kw
Rated voltage	400	V
Rated torque	10	Nm
Stator resistance (Rs)	3.32	Ω
Rotor resistance (Rr)	2.11	Ω
Stator leakage inductance (Lls)	0.00439	mH
Rotor leakage inductance (Llr)	0.00439	mH
Mutual inductance (Lm)	0.2373	mH
Stator flux linkage (ψs)	0.9	Wb
Motor Moment of Inertia (J)	0.01	kg-m2
Number of poles	2	P

the result came out that the PSO overwhelmed the second proposed GA scheme. The drawback of this scope is that the expectation of flux ripples has not been reduced enough because both proposed schemes were focused on the error and change of error for the torque signal only.

Future work will explore on how to accurately control the proposed method to reduce the torque ripples and how to further design more robust DTC strategy when taking into account the error and change of error for both flux and torque by means of intelligent techniques.

CRediT authorship contribution statement

Mohamed Elgbaily: Conceptualization, Methodology, Software, Validation, Formal analysis, Investigation, Resources, Data curation, Writing – original draft, Writing – review & editing, Visualization, Project administration, Funding acquisition. **Fatih Anayi:** Conceptualization, Validation, Formal analysis, Investigation, Resources, Data curation, Writing – review & editing, Supervision, Project administration. **Michael Packianather:** Software, Investigation, Resources, Data curation, Writing – review & editing, Supervision.

Data availability

No data was used for the research described in the article.

Declaration of Competing Interest

The authors declare that they have no known competing financial interests or personal relationships that could have appeared to influence the work reported in this paper.

Acknowledgement

This work was carried out with the aid of a grant from the Ministry of Higher Education and Scientific Research in Libya, provided through Libyan Cultural Affairs London in the UK.

Appendix A. Induction motor parameters

(See Table 6.).

References

[1] H. Shayeghi, A. Ahmadpour, M.M.H.K. Heiran, Optimal operation of wind farm in presence of pumped-storage station as smart infrastructure and load estimation using artificial neural networks, in: In 2017 Smart Grid Conference (SGC), 2017, pp. 1–7.
[2] Y. Yue, Q. Xu, A. Luo, P. Guo, Z. He, Y. Li, Analysis and control of tundish induction heating power supply using modular multilevel converter, IET Gener. Transm. Distrib. 12 (14) (2018) 3452–3460.
[3] E. El-Kharashi, J.G. Massoud, Approach to measure the degree of the unbalanced power in induction motor for energy-efficient use, J. Eng. 2017 (8) (2017) 452–465.
[4] J. Guo, X. Ma, A. Ahmadpour, Electrical–mechanical evaluation of the multi–cascaded induction motors under different conditions, Energy 229 (2021), https://doi.org/10.1016/j.energy.2021.120664 120664.
[5] M. Hasanuzzaman, N.A. Rahim, R. Saidur, S.N. Kazi, Energy savings and emissions reductions for rewinding and replacement of industrial motor, Energy 36 (1) (2011) 233–240.
[6] P. Waide and C. U. Brunner, "Energy-efficiency policy opportunities for electric motor-driven systems," 2011.
[7] A.C.A. Chikhi, A comparative study of field-oriented control and direct-torque control of induction motors using an adaptive flux observer, J. Electr. Eng. 10 (3) (2010) 7.
[8] D. Casadei, F. Profumo, G. Serra, A. Tani, FOC and DTC: two viable schemes for induction motors torque control, IEEE Trans. Power Electron. 17 (5) (2002) 779–787.
[9] H.M. Boulouiha, A. Allali, M. Laouer, A. Tahri, M. Denai, A. Draou, Direct torque control of multilevel SVPWM inverter in variable speed SCIG-based wind energy conversion system, Renew. Energy 80 (2015) 140–152.
[10] A. Haddoun, M.E.H. Benbouzid, D. Diallo, R. Abdessemed, J. Ghouili, K. Srairi, "Comparative analysis of control techniques for efficiency improvement in electric vehicles", IEEE Vehicle Power Propul. Conf. 2007 (2007) 629–634.
[11] N. El Ouanjli, A. Derouich, A. El Ghzizal, A. Chebabhi, M. Taoussi, "A comparative study between FOC and DTC control of the doubly fed induction motor (DFIM)", Int. Conf. Electric. Information Technol. (ICEIT) 2017 (2017) 1–6.
[12] I. Takahashi, T. Noguchi, A new quick-response and high-efficiency control strategy of an induction motor, IEEE Trans. Ind. Appl. 5 (1986) 820–827.
[13] M. Depenbrock, Direct self-control (DSC) of inverter-fed induction machine, IEEE Trans. Power Electron. 3 (4) (1988) 420–429, https://doi.org/10.1109/63.17963.
[14] U. Senthil and B. G. Fernandes, "Hybrid space vector pulse width modulation based direct torque controlled induction motor drive," in *IEEE 34th Annual Conference on Power Electronics Specialist, 2003. PESC '03.*, 2003, vol. 3, pp. 1112–1117 vol.3, doi: 10.1109/PESC.2003.1216605.
[15] J.-K. Kang, S.-K. Sul, New direct torque control of induction motor for minimum torque ripple and constant switching frequency, IEEE Trans. Ind. Appl. 35 (5) (1999) 1076–1082, https://doi.org/10.1109/28.793368.
[16] C.A. Martins, X. Roboam, T.A. Meynard, A.S. Carvalho, Switching frequency imposition and ripple reduction in DTC drives by using a multilevel converter, IEEE Trans. Power Electron. 17 (2) (2002) 286–297.
[17] K.-B. Lee, J.-H. Song, I. Choy, J.-Y. Yoo, Torque ripple reduction in DTC of induction motor driven by three-level inverter with low switching frequency, IEEE Trans. Power Electron. 17 (2) (2002) 255–264.
[18] T.G. Habetler, F. Profumo, M. Pastorelli, L.M. Tolbert, Direct torque control of induction machines using space vector modulation, IEEE Trans. Ind. Appl. 28 (5) (1992) 1045–1053.
[19] E. Flach, R. Hoffmann, P. Mutschler, Direct mean torque control of an induction motor, Eur. Conf. Power Electron. App. 3 (1997) 3–672.
[20] S.M. Gadoue, D. Giaouris, J.W. Finch, Artificial intelligence-based speed control of DTC induction motor drives—a comparative study, Electr. Power Syst. Res. 79 (1) (2009) 210–219.
[21] M. Valipour, Optimization of neural networks for precipitation analysis in a humid region to detect drought and wet year alarms, Meteorol. Appl. 23 (1) (2016) 91–100.
[22] O. Ouledali, A. Meroufel, P. Wira, S. Bentouba, Direct torque fuzzy control of PMSM based on SVM, Energy Procedia 74 (2015) 1314–1322.
[23] M. Elgbaily, F. Anayi, M. Packianather, "Performance improvement based torque ripple minimization for direct torque control drive fed induction motor using fuzzy logic control", Control, Instrument. Mech.: Theor. Pract., Springer (2022) 416–428.
[24] T.Y. Abdalla, H.A. Hairik, A.M. Dakhil, Direct torque control system for a three phase induction motor with fuzzy logic based speed Controller, in: In 2010 1st International Conference on Energy, Power and Control (EPC-IQ), 2010, pp. 131–138.
[25] T. Ramesh, A. Kumar Panda, S. Shiva Kumar, Type-2 fuzzy logic control based MRAS speed estimator for speed sensorless direct torque and flux control of an induction motor drive, ISA Trans. 57 (2015) 262–275, https://doi.org/10.1016/j.isatra.2015.03.017.
[26] G.-M. Sung, W.-Y. Wang, W.-S. Lin, and C.-P. Yu, "Predictive Direct Torque Control Application-Specific Integrated Circuit of an Induction Motor Drive with a Fuzzy Controller," J. Low Power Electron. Appl., vol. 7, no. 2, 2017, doi: 10.3390/jlpea7020015.
[27] S. H., K. S.F., and S. B., "Improvements in direct torque control of induction motor for wide range of speed operation using fuzzy logic," J. Electr. Syst. Inf. Technol., vol. 5, no. 3, pp. 813–828, 2018, doi: https://doi.org/10.1016/j.jesit.2016.12.015
[28] S.G. Malla, A review on Direct Torque Control (DTC) of induction motor: With applications of fuzzy, in: In 2016 International Conference on Electrical, Electronics, and Optimization Techniques (ICEEOT), 2016, pp. 4557–4567, https://doi.org/10.1109/ICEEOT.2016.7755579.
[29] V.M.V. Rao, A.A. Kumar, Artificial Neural Network and Adaptive Neuro Fuzzy Control of Direct Torque Control of Induction Motor for Speed and Torque Ripple Control, in: in 2018 2nd international Conference on Trends in

Electronics and Informatics (ICOEI), pp. 1416–1422, https://doi.org/10.1109/ICOEI.2018.8553871.
[30] T. Ahammad, A.R. Beig, K. Al-Hosani, "An improved direct torque control of induction motor with modified sliding mode control approach", Int. Electric Mach. Drives Conf. 2013 (2013) 166–171, https://doi.org/10.1109/IEMDC.2013.6556249.
[31] C. Lascu, A. Argeseanu, F. Blaabjerg, Supertwisting sliding-mode direct torque and flux control of induction machine drives, IEEE Trans. Power Electron. 35 (5) (2020) 5057–5065, https://doi.org/10.1109/TPEL.2019.2944124.
[32] A.N. Abdullah, M.H. Ali, Direct torque control of IM using PID controller, Int. J. Electr. Comput. Eng. 10 (1) (2020) 617.
[33] P. Tiitinen, M. Surandra, The next generation motor control method, DTC direct torque control, Proc. Int. Conf. Power Electron., Drives Energy Syst. Industrial Growth 1 (1996) 37–43.
[34] J.-S. Kim, J.-H. Kim, J.-M. Park, S.-M. Park, W.-Y. Choe, H. Heo, Auto tuning PID controller based on improved genetic algorithm for reverse osmosis plant, World Acad. Sci. Eng. Technol. 47 (2) (2008) 384–389.
[35] L. Davis, "Handbook of genetic algorithms," 1991.
[36] J. Kennedy and R. Eberhart, "Particle swarm optimization," in *Proceedings of ICNN'95-international conference on neural networks*, 1995, vol. 4, pp. 1942–1948
[37] Y. Marinakis, M. Marinaki, A hybrid genetic–particle swarm optimization algorithm for the vehicle routing problem, Expert Syst. Appl. 37 (2) (2010) 1446–1455.
[38] B. Samanta, C. Nataraj, Use of particle swarm optimization for machinery fault detection, Eng. Appl. Artif. Intell. 22 (2) (2009) 308–316.
[39] R.-J. Wai, Y.-F. Lin, K.-L. Chuang, Total sliding-mode-based particle swarm optimization control for linear induction motor, J. Franklin Inst. 351 (5) (2014) 2755–2780.
[40] Z.-L. Gaing, A particle swarm optimization approach for optimum design of PID controller in AVR system, IEEE Trans. Energy Convers. 19 (2) (2004) 384–391.
[41] A. Humod and W. Jabbar, "Direct Torque control of induction motor based on Particle Swarm Optimization," *J. Al-Rafidain Univ. Coll. Sci. (Print ISSN 1681-6870, Online ISSN 2790-2293)*, no. 2, pp. 87–108, 2013.